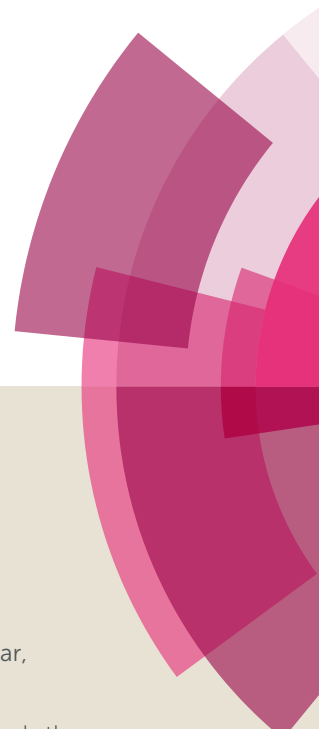


NJC

Accepted Manuscript



This article can be cited before page numbers have been issued, to do this please use: S. G. R. M. Borkar, S. U. M. Kanakaraju, G. Saicharan, S. Misra and S. R., *New J. Chem.*, 2019, DOI: 10.1039/C9NJ00932A.



This is an Accepted Manuscript, which has been through the Royal Society of Chemistry peer review process and has been accepted for publication.

Accepted Manuscripts are published online shortly after acceptance, before technical editing, formatting and proof reading. Using this free service, authors can make their results available to the community, in citable form, before we publish the edited article. We will replace this Accepted Manuscript with the edited and formatted Advance Article as soon as it is available.

You can find more information about Accepted Manuscripts in the [author guidelines](#).

Please note that technical editing may introduce minor changes to the text and/or graphics, which may alter content. The journal's standard [Terms & Conditions](#) and the ethical guidelines, outlined in our [author and reviewer resource centre](#), still apply. In no event shall the Royal Society of Chemistry be held responsible for any errors or omissions in this Accepted Manuscript or any consequences arising from the use of any information it contains.

1
2
3 **Identification and structural characterization of stress degradation products of omeprazole**
4
5 **using Q-TOF-LC-ESI-MS/MS and NMR experiments: Evaluation of toxicity of**
6
7 **degradation products**
8
9

10 **G. Shankar^a, Roshan M. Borkar^a, Suresh Udutha^a, M. Kanakaraju^b, G. Sai Charan^b,**

11
12
13 **S Misra^c, R. Srinivas^{*a}**
14

15
16 ^{a,b}*Analytic chemistry, CSIR-Indian Institute of Chemical Technology, Hyderabad, 500 007, India*

17
18 ^c*Biology Division, CSIR-Indian Institute of Chemical Technology, Hyderabad, 500007, India*
19
20

21
22
23
24
25
26 **Keywords:** omeprazole, degradation products, accurate mass measurements, *in vitro* and *in*
27
28 *silico* toxicity
29
30

31
32
33
34 ^{a,b*} Corresponding author : srini@iict.res.in (R. Srinivas)

35
36
37
38 sragampeta@yahoo.co.in

39
40
41 Telephone Number : +91-40-27193122

42
43
44 Fax Number : +91-40-27193156
45
46
47
48
49

50 Manuscript Number: IICT/Pubs./2018/388
51
52
53
54
55
56
57
58
59
60

Abstract

Omeprazole (OMP), a prototype proton pump inhibitor used for the treatment of peptic ulcers and gastroesophageal reflux disease (GERD), was subjected to forced degradation studies as per ICH guidelines Q1A (R2). The drug undergoes degradation under acid, base, neutral hydrolysis and oxidative degradation conditions and forms a total of sixteen degradation products which were characterized by LC-MS/MS experiments and accurate mass measurements. Oxidative degradation products (OMP-15 and OMP-16) were synthesized and confirmed by various NMR experiments. The cytotoxic effects of OMP-15 and OMP-16 were tested on normal human cells such as HEK 293 and NIH3T3 by MTT assay. Based on the cytotoxicity results, compared to the standard OMP, both OMP-15 and OMP-16 were found to have relatively lesser toxic effects towards normal cells. Further, *in silico* toxicity of OMP and its degradation products (OMP-1 to OMP-16) were assessed by ProTox-II prediction tool. OMP and OMP-8 are predicted for carcinogenicity, OMP-7 for hepato toxicity and OMP-2, OMP-3, OMP-9, OMP-11, OMP-14 and OMP-16 for immune system with high confidence score. The drug, OMP-1, OMP-6, OMP-7, OMP-8, OMP-13 and OMP-15 are predicted to combine with aryl hydro carbon receptor (AhR) with high probability score. Additionally, two different targets, Amine Oxidase A and Prostaglandin G/H Synthase 1 are predicted as toxicity targets for OMP, OMP-1, OMP-6, OMP-8, OMP-13, OMP-15 and OMP-16 with probable binding.

1. Introduction

Stress degradation is the process for examining the stability of drug molecules in the presence of chemical and environmental conditions to determine the product breakdown levels. According to the ICH guidelines stress testing is a process for identification of degradation products and it will further help to determine the inherent stability of the drug molecule [1]. Stress testing

1
2
3 provides information about degradation pathways and potential degradation products.
4
5 Identification and structural characterization of degradation products is useful to establish the
6
7 mechanism of formation of degradation products from the drug and to know the toxicity
8
9 information and side effects of drug [2]. Identification of low level of unknown degradation
10
11 products and impurities can be challenging [3]. There are many reports in the literature on
12
13 structural elucidation of degradation products of various pharmaceutical drugs using LC-MS/MS
14
15 experiments [4-8].
16
17

18
19 All the drug substances and drug products tends to degrade over the timeframe affected by the
20
21 factor such as light, pH, moisture, heat etc. Considering these factors International Conference
22
23 on Harmonization (ICH) guideline has brought protocols in a harmonized way [9]. Formation of
24
25 degradation products can also be formed by hydrolysis, oxidation, dimerization, rearrangement,
26
27 adduct formation and the combination of these processes [10].
28
29

30
31 The identified and characterized degradation products can be subjected to toxicity studies for risk
32
33 assessment of potentially genotoxic degradation products. Evaluation of toxicity of degradation
34
35 products is important from the safety and efficacy point of view as per ICH guideline Q3A and
36
37 Q3B [11,12]. There are several examples in the literature on the adverse effects of degradation
38
39 products of various drugs. For example severe adverse effects of the degradation products of
40
41 tetracycline and aminopencillins have been reported [13,14]. Degradation products can lead to
42
43 carcinogenicity due to genetic mutations, chromosomal breaks, and/or chromosomal
44
45 rearrangements [15] Recently, we have reported in *vitro* and *in silico* toxicity of degradation
46
47 products of lansoprazole, rabeprazole and sumatriptan succinate [16-18].
48
49

50
51 Gastroesophageal reflux disease (GERD) is a common chronic disorder, which is characterized
52
53 by increased reflux of gastric contents into the lower esophagus [19,20]. The severity of GERD
54
55
56
57
58
59
60

1
2
3 is directly correlated with the degree and duration of esophageal acid exposure and is highly pH
4 dependent [21,22]. Severe reflux esophagitis may convert to serious complications like
5 esophageal structure and Barrett's esophagus in patients with GERD [23,24].
6
7

8
9
10 Proton pump inhibitors (PPIs) are the most widely prescribed medication to reduce gastric acid
11 secretion. Omeprazole (OMP), 5-methoxy-2-[[[4-methoxy-3,5-dimethyl-2-pyridinyl) methyl]
12 sulphanyl]-1H-benzo [d] imidazole, is widely used for the treatment of peptic ulcers,
13 Gastroesophageal Reflux Disease (GERD), dyspepsia and Zollinger–Ellison syndrome [25].
14 OMP is the first clinically used prototypical proton pump inhibitor, subsequently lansoprazole,
15 pantoprazole, rabeprazole and the stereo-isomeric drug substances esomeprazole and
16 dexlansoprazole were introduced [26]. Long-term OMP therapy is highly effective and more safe
17 for control of reflux esophagitis [27].
18

19
20 Several analytical methods have been reported for determination of OMP and its impurities in
21 bulk drug and formulations [28-30]. Few HPLC and LC MS methods have been reported for
22 determination of OMP and its metabolites in plasma [31-33]. However, no study exists on
23 systematic stress degradation study of OMP as per ICH guidelines. Hence, the main aim of this
24 study is to identify and characterize the degradation products of OMP. This was done by
25 exposing the drug to ICH-recommended stress conditions of hydrolysis, oxidation, thermal and
26 photolysis. The resultant solutions were subjected to optimized LC-MS/MS experiments to
27 establish the fragmentation pattern of the drug and its degradation products. Further we
28 synthesized the oxidative degradation products and confirmed their structures by 1D, 2D NMR
29 experiments prior to evaluating their *in vitro* toxicity. In addition, we have studied the *in silico*
30 toxicities of all the degradation products.
31
32
33
34
35
36
37
38
39
40
41
42
43
44
45
46
47
48
49
50
51
52
53
54
55
56
57
58
59
60

2. Experimental

2.1 Chemicals and reagents

Omeprazole (OMP), methanol-d₄, tris hydrochloride (Tris-HCl), 3-(4,5-Dimethyl-2-thiazolyl)-2,5-diphenyl-2H-tetrazolium bromide and Deoxyribonucleic acid from calf thymus (ctDNA) was purchased from Sigma Aldrich, India. HPLC Grade acetonitrile (ACN) and methanol (MeOH) were purchased from Merck, India. HPLC grade water was prepared by filtrating through a Millipore Milli-Q- plus system (Millipore, Milford, MA, USA). Ammonium acetate of HPLC grade was purchased from Finar Chemicals Pvt. Ltd. (Ahmedabad, India). All analytical grade reagents, formic acid, sodium hydroxide, hydrochloric acid, dichloromethane (DCM) and 30% hydrogen peroxide were purchased from Merck (Mumbai, India).

2.2. Instrumentation

2.2.1. Liquid Chromatography-Mass spectrometry

The Agilent 1290 infinity series LC system (Agilent technologies, USA) consisting of an auto sampler (G7129B), a quaternary pump (G7104A), a diode array detector (G7117A), a column compartment (G7116B) and a degasser was employed for HPLC analysis. LC/MS analysis was performed on a Ultra Performance liquid chromatography (UPLC) coupled to a quadrupole time-of-flight mass spectrometer (Q-TOF LC/MS 6545 series- G6545A, Agilent Technologies, USA). Acquisition of the data was under the control of Mass Hunter workstation software.

The fragmentation pathway of OMP was established by carrying out Q-TOF-MS/MS. ESI source was operated in positive ionization mode with a capillary voltage of 3000-3500 V and skimmer at 60 V. Collision gas used for mass experiments was ultrahigh pure nitrogen and 30 eV energy was used for MS/MS studies. Nitrogen was used as the drying (325°C, 10 Lmin⁻¹) and nebulizing (45 psi) gas. Mass-Hunter Workstation software was used for the data processing of

total ion chromatograms (TICs) and to determine the elemental composition from accurate mass measurements of m/z values.

2.2.2. Nuclear magnetic resonance spectroscopy

The degradation products (OMP-15 and OMP-16) were analysed by various NMR techniques (^1H , ^{13}C and 2D). Chemical shift values on δ scale in ppm were measured at 400MHz frequency by using NMR spectroscopy (AVANCE III HD-400, Bruker, Billerica, Massachusetts, United States). Tetra methyl silane (TMS) is used as internal standard and adjusted to 0 ppm on δ scale. The data acquisition and processing of NMR spectra was done using Top spin software (3.2version).

2.3. Stressed degradation conditions

Stress degradation studies of OMP were carried out on the bulk drug as per ICH guidelines Q1A (R2). The drug solutions were prepared in 1.0 mg/mL concentration for all the stressed reactions. Acidic hydrolysis of the drug was carried out by using 0.01N HCl at room temperature for 30 min. Whereas, basic and neutral hydrolysis were conducted by refluxing the drug in 2N NaOH and water at 80°C under reflux for 48 h and 24 h, respectively. For oxidative degradation study, the drug was subjected to 3% H_2O_2 at room temperature for 24 h. Photolytic studies were performed by exposing solid and solution of the drug sample to 1.2×10^6 lux h of fluorescent light and 200W h m^{-2} UV light in a photo stability chamber. For thermal degradation study, the drug sample was sealed in glass vial and kept in a thermostatic block at 80°C for 1week. All stressed samples were kept in a refrigerator at 4°C until analysis.

2.4. Sample preparation

All the stressed samples (hydrolytic, oxidative, thermal and photolytic) were collected and

neutralized. All solutions were filtered through 0.22 μm pore size membrane syringe filter before LC-MS/MS analysis.

2.5. Analysis of stressed samples

2.5.1. Method development and optimization of LC-MS conditions

The chromatographic conditions were optimized using Hiber Purospher, C18 (250 X 4.6mm, 5 μ) (Merck Lichro, Switzerland) column with a mobile phase composed of 10 mM ammonium acetate(A) and ACN(B) in gradient elution mode. The linear gradient programme was set as follows: (T_{min} /% proportion of solvent B): 0-5/10, 5-7/30, 7-14/ 40, 14-20/45, 20-30/ 45, 30-35/ 50, 35-40/85, 40-42/10, 42-44/10. The column temperature, flow rate, injection volume, and detector wavelength were at 30 $^{\circ}\text{C}$, 1.0 ml/min, 20.0 μl , and 302 nm, respectively. The typical operating source conditions for MS scan in positive ion ESI mode were optimized as follows; the fragmentor voltage was set at, 120 V; the capillary at, 3000–3500 V; sheath gas temp at, 350 $^{\circ}\text{C}$; flow of sheath gas at, 11 L/min; nebulizing (45 psi) gas and nitrogen was used as the drying (250 $^{\circ}\text{C}$; 13 L/min). For full scan MS mode, the mass range was set at m/z 50–1000.

For collision-induced dissociation(CID) experiments, keeping MS¹ static, interested precursor ion was selected using the quadrupole analyzer, and the product ions were analyzed by a time-of-flight (TOF) analyzer. Ultrahigh pure nitrogen was used as collision gas.

2.6 Chemical synthesis

The mono and di oxidative degradation products of OMP (OMP-15, OMP-16) were obtained by the synthesis. OMP was used as a starting material and *meta*- Chloroperoxybenzoic acid (*m*-CPBA) as a reagent. The reagent *m*-CPBA (172mg, 1 mmol for OMP-15 and 2 mmol for OMP-16) was added to a solution of OMP (345 mg, 1.0 mmol) in 3 ml of DCM at 0 $^{\circ}\text{C}$ and the reaction mixture was stirred overnight at room temperature. The reaction mixture was quenched

with sodium bicarbonate followed by extraction with ethyl acetate. After extraction, the residue was purified by using silica gel column chromatography (DCM–MeOH, 9.5:0.5 %) to get the pure products as white solid. The samples were characterized by 1D, 2D-NMR experiments using deuterated methanol (CD₃OD).

2.7. *In vitro* toxicity evaluation

2.7.1. *In vitro* 3-(4, 5-dimethylthiazol-2-yl)-2, 5-diphenyl tetrazolium bromide (MTT) assay

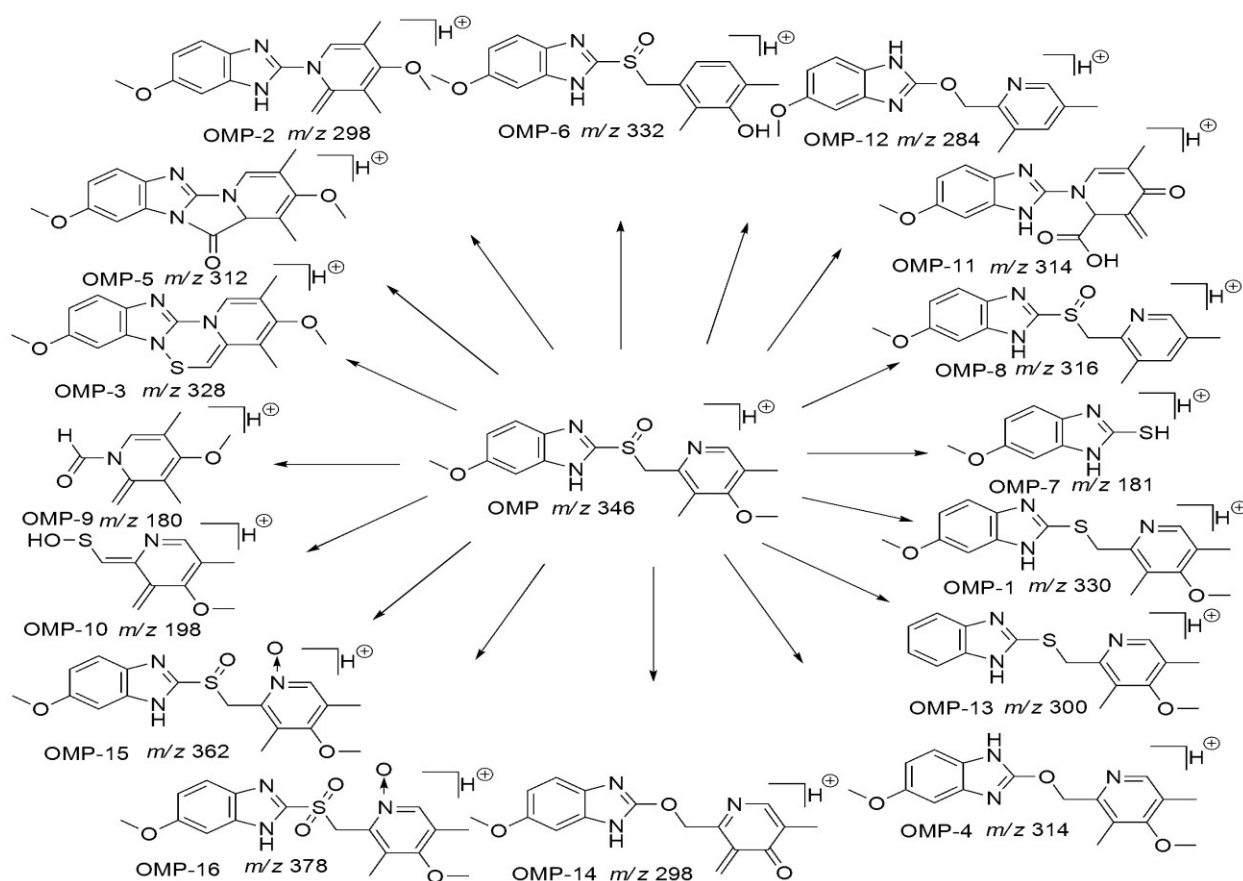
Cytotoxicity assay (MTT) was evaluated for all the test compounds as per our earlier published work (Bollu et al., 2016) [34]. Two different normal cell lines viz., Normal human embryonic kidney cells (HEK-293) and Normal mouse embryo fibroblast cells (NIH3T3) were obtained from the ATCC (Bethesda, MD, USA) and maintained in DMEM supplemented with 10 % FBS, 2 mM l-glutamine, 100 U/ml penicillin, and 100 µg/ml streptomycin at 37 °C in a 5 % CO₂ incubator. After seeding of cells in 96 well flat bottom tissue culture plate and test compounds of different concentrations ranging from 1 to 100 µg were added in triplicates and incubated for 48hr. The cells were then incubated with MTT (0.5 mg/mL) for 3h and 100 µl DMSO was added to each well to dissolve the insoluble formazan crystals. Finally the absorbance of the plates were measured using a Synergy H1 multi-mode plate reader, USA. OMP was used as positive control for the comparison.

3. Results and discussion

3.1 Degradation behaviour of the OMP

The degradation behaviour of OMP was analyzed using LC/MS under stress degradation conditions as per ICH guidelines. The optimized LC/MS method was used for identification of OMP degradation products. The drug was found to be degraded in acid, base, neutral hydrolysis

and oxidation degradation conditions. Whereas it was found to be stable under thermal and photolytic conditions. Totally **16** degradation products of OMP were identified and characterized by using LC-MS/MS. The elemental compositions of OMP degradation products and their product ions have been confirmed by accurate mass measurements. Structure of the degradation products was proposed based on the MS/MS fragmentation data of the drug and degradation products. The proposed structures of degradation products of OMP and their elemental compositions are given in **scheme 1** and **table 1**, respectively.



Scheme 1: Proposed structures of protonated degradation products of OMP.

3.2.1 Hydrolysis

The LC/ESI/HRMS analysis of OMP (**Figure 1(a)**), in acid hydrolysis showed an extensive degradation and formed five degradation products (OMP-1, OMP-2, OMP-3, OMP-4, OMP-5)

(Figure 1(b)). In the case of base hydrolysis (Figure 1(c)) six degradation products (OMP-1, OMP-6, OMP-7, OMP-8, OMP-9, OMP-10) were formed, whereas in neutral condition (Figure 1(d)) seven degradation products (OMP-2, OMP-5, OMP-8, OMP-11, OMP-12, OMP-13, OMP-14) formed, respectively.

Table 1: Elemental composition of protonated degradation products of OMP

Degradation Products	Rt (min)	Formula	Observed (m/z)	Calculated (m/z)	Error (ppm)
OMP-1	27.39	C ₁₇ H ₂₀ N ₃ O ₂ S ⁺	330.1260	330.1270	3.02
OMP-2	14.43	C ₁₇ H ₂₀ N ₃ O ₂ ⁺	298.1528	298.1550	0.67
OMP-3	18.33	C ₁₇ H ₁₈ N ₃ O ₂ S ⁺	328.1116	328.1114	-0.60
OMP-4	22.34	C ₁₇ H ₂₀ N ₃ O ₃ ⁺	314.1511	314.1499	-3.81
OMP-5	18.66	C ₁₇ H ₁₈ N ₃ O ₃ ⁺	312.1337	312.1342	1.60
OMP-6	11.50	C ₁₆ H ₁₈ N ₃ O ₃ S ⁺	332.1052	332.1063	3.91
OMP-7	13.05	C ₈ H ₉ N ₂ OS ⁺	181.0404	181.0430	-2.20
OMP-8	14.07	C ₁₆ H ₁₈ N ₃ O ₂ S ⁺	316.1094	316.1114	4.74
OMP-9	18.29	C ₁₀ H ₁₄ NO ₂ ⁺	180.1016	180.1019	1.66
OMP-10	20.68	C ₉ H ₁₂ NO ₂ S ⁺	198.0576	198.0583	3.53
OMP-11	10.66	C ₁₆ H ₁₆ N ₃ O ₄ ⁺	314.1138	314.1135	-0.95
OMP-12	14.70	C ₁₆ H ₁₈ N ₃ O ₂ ⁺	284.1378	284.1393	5.27
OMP-13	23.17	C ₁₆ H ₁₈ N ₃ O ₃ ⁺	300.1341	300.1342	0.33
OMP-14	23.97	C ₁₆ H ₁₆ N ₃ O ₃ ⁺	298.1174	298.1186	4.02
OMP-15	20.02	C ₁₇ H ₂₀ N ₃ O ₄ S ⁺	362.1152	362.1169	4.69
OMP-16	15.14	C ₁₇ H ₂₀ N ₃ O ₅ S ⁺	378.1102	378.1118	4.23

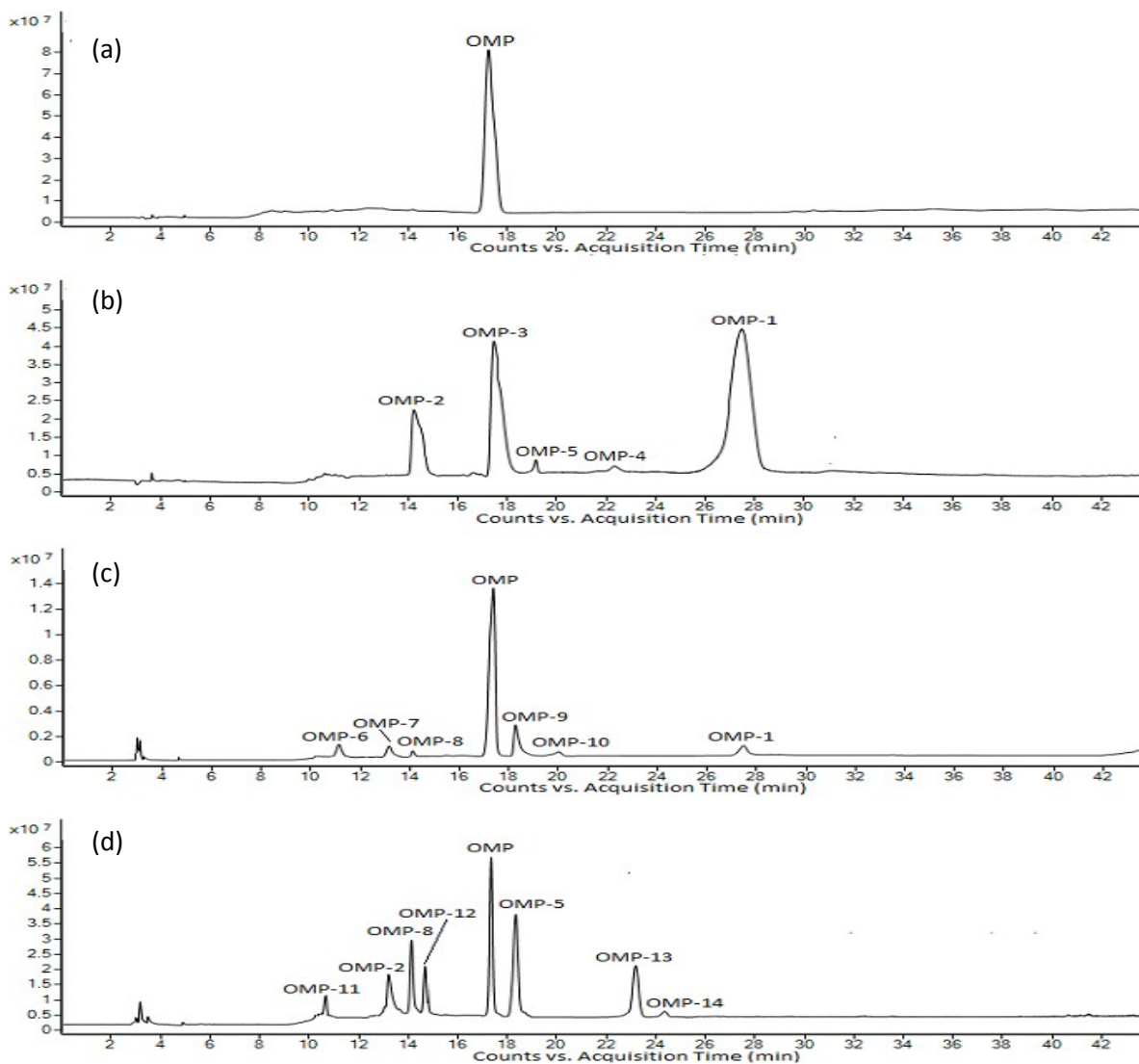


Figure.1. UPLC/ESI/MS TICs of OMP(a) and its degradation products under acid (b), base (c), and neutral (d) hydrolytic conditions.

3.2.2. Oxidation

A total of three degradation products (OMP-2, OMP-15, OMP-16) of OMP were formed, when it was subjected to 3% H_2O_2 at room temperature for 24 hr. (Figure. 2(a)).

3.2.3. Thermal degradation

The OMP was found to be stable under thermal condition after the exposures of 1 week at 80 °

C. (Figure. 2(b))

3.2.4. Photolytic degradation

The drug was found to be stable under UV and fluorescence degradation conditions after the exposures of 1 week. (Figure.2(c))

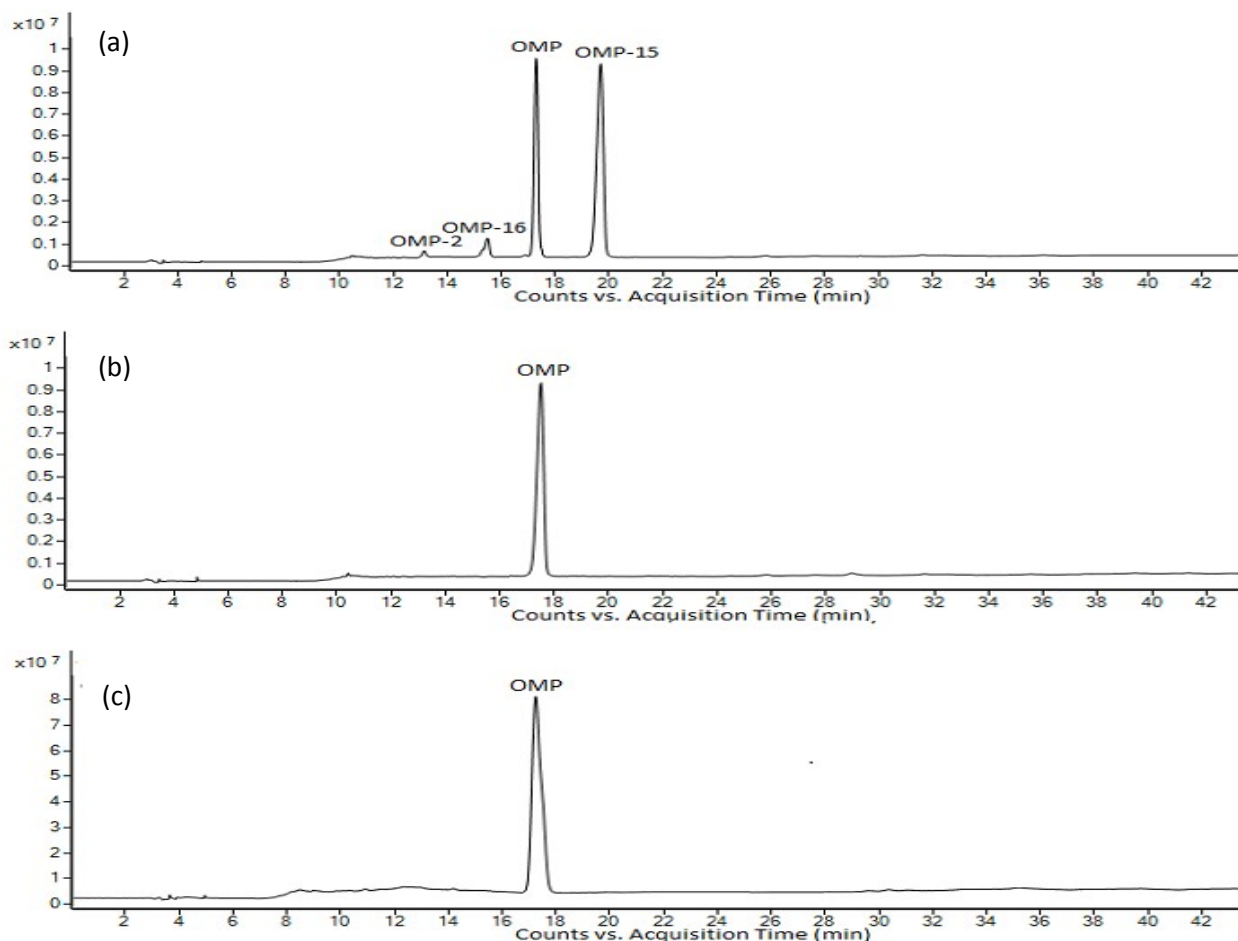


Figure.2. UPLC/ESI/MS TICs of OMP degradation products under oxidation (a), thermal (b) and photolytic (c) condition

4. MS/MS study of the protonated drug and its degradation products

4.1 OMP ($[M+H]^+$, m/z 346.1233)

The fragmentation pathway of the drug was established by using LC-MS/MS combined with accurate mass measurements. The protonated drug at m/z 346 ($[M+H]^+$) with an elemental composition $C_{19}H_{23}FN_3O_4^+$ was eluted at 17.36 min. (**Figure.1(a)**) The LC-MS/MS spectrum of $[M+H]^+$ of OMP showed high abundance product ion at m/z 198 (loss of $C_8H_8N_2O$) and low abundance product ions at m/z 328 (loss of H_2O), m/z 295 (loss of SH radical from m/z 328), m/z 180 (loss of H_2O from m/z 198), m/z 168 (loss of $C_8H_6N_2OS$), m/z 151 (loss of OH radical from m/z 168), m/z 149 (loss of $C_9H_{11}NO_2S$), m/z 136 (loss of CH_3OH from m/z 168), m/z 121 (loss of CH_2O from m/z 151) and m/z 79 (loss of C_2H_4N radical). The product ion at m/z 149 is characteristic ion for 5-methoxy-1*H*-benzo[*d*]imidazole skeleton and m/z 168, m/z 151, m/z 136 and m/z 121 are significant ions for 4-methoxy-3,5-dimethylpyridine. (**Supplementary Scheme S1, Figure S1(a), see Supporting Information**) The product ions at m/z 328, m/z 295, m/z 198 and m/z 180 indicates the presence of sulphur monoxide linked to 5-methoxy-1*H*-benzo[*d*]imidazole skeleton and 4-methoxy-3,5-dimethylpyridine. The elemental compositions of all these ions have been confirmed by accurate mass measurements. (**Supplementary Table.S1, see Supporting Information**)

4.2 MS/MS study of degradation products

OMP-1 ($[M+H]^+$, m/z 330.1260)

The degradation product OMP-1 at m/z 330 ($[M+H]^+$) with an elemental composition $C_{17}H_{20}N_3O_2S^+$ detected at 27.39 min in acid and base hydrolysis conditions. The decrease of 16 Da in molecular weight compared to the $[M+H]^+$ of the drug suggests that OMP-1 was formed by loss of 'O' atom from the drug. The LC-MS/MS spectrum of OMP-1 showed high abundance

product ion at m/z 182 (loss of 5-methoxy-1*H*-benzo[*d*]imidazole) and low abundance product ions at m/z 297 (loss of SH radical), m/z 267 (loss of CH₂O from m/z 297), m/z 166 (loss of CH₄ from m/z 182), m/z 151 (loss of CH₃ radical from m/z 166), m/z 150 (loss of C₈H₈N₂OS), m/z 149 (loss of C₉H₁₁NOS), m/z 136 (loss of CH₂S from m/z 182) and m/z 120 (loss of CH₂O from m/z 150). The diagnostic product ions at m/z 182 and m/z 149 supports the proposed structure of OMP-1. The product ions at m/z 295, m/z 280 and m/z 180 are characteristic ions for OMP-1. **(Supplementary Scheme.S2, Figure S1(b) Table.S2, see Supporting Information)** Based on these data, OMP-1 was identified as 5-methoxy-2-((4-methoxy-3,5-dimethylpyridin-2-yl)methylthio)-1*H*-benzo[*d*]imidazole.

OMP-2 ([M+H]⁺, m/z 298.1528)

The degradation product OMP-2 at m/z 298 ([M+H]⁺) with an elemental composition C₁₇H₂₀N₃O₂⁺ detected at 14.43 min in acidic, neutral hydrolytic and oxidation conditions. The LC-MS/MS spectrum of [M+H]⁺ of OMP-2 showed high abundance product ion at m/z 268 (loss of CH₃ radical from m/z 283) and low abundance product ions at m/z 283 (loss of CH₃ radical), m/z 282 (loss of CH₄), m/z 266 (loss of CH₃OH), m/z 254 (loss of CO from m/z 282), m/z 253 (loss of CH₃ radical from m/z 268), m/z 240 (loss of CO from m/z 268), m/z 151 (loss of C₈H₇N₂O radical), m/z 150 (loss of C₈H₈N₂O) and m/z 147 (loss of C₉H₁₃NO). The diagnostic product ions at m/z 147 and m/z 150 supports the proposed structure of OMP-2. **(Supplementary Scheme S3, Figure S1(c), Table.S2, see Supporting Information)** Based on these data OMP-2 was identified as 5-methoxy-2-(4-methoxy-3,5-dimethyl-2-methylenepyridin-1(2*H*)-yl)-1*H*-benzo[*d*]imidazole.

OMP-3 ([M+H]⁺, m/z 328.1116)

The degradation product OMP-3 at m/z 328 ([M+H]⁺) with an elemental composition C₁₇H₁₈N₃O₂S⁺ detected at 18.33 min in acid hydrolytic condition. The mass difference between the protonated drug (m/z 346) and OMP-3 (m/z 328) is 18 u which suggests that OMP-3 was formed by loss of H₂O from the drug. The LC-MS/MS spectrum of [M+H]⁺ of OMP-3 showed high abundance product ions at m/z 280 (loss of 'S' from m/z 312), m/z 120 (loss of CH₂O from m/z 150), m/z 106 (loss of CH₂O from m/z 136) and low abundance ions at m/z 312 (loss of CH₄), m/z 298 (loss of C₂H₆), m/z 295 (loss of SH radical), m/z 284 (loss of CO from m/z 312), m/z 280 (loss of 'S' from m/z 312), m/z 265 (loss of CH₃ radical from m/z 280) and m/z 180 (loss of C₈H₈N₂O). The characteristic product ions at m/z 295, m/z 280 and m/z 180 supports the proposed structure of OMP-3. (**Supplementary Scheme.S4, Figure S1(d), Table.S3, see Supporting Information**). Based on all these data, OMP-3 structure was proposed as shown in **Scheme. 1**.

OMP-4 ([M+H]⁺, m/z 314.1511)

The acid hydrolytic degradation product OMP-4 at m/z 314 ([M+H]⁺) with an elemental composition C₁₇H₂₀N₃O₃⁺ detected at 22.34 min. The LC-MS/MS spectrum of [M+H]⁺ of OMP-4 showed high abundance product ion at m/z 120 (loss of CH₂O from m/z 150) and low abundance product ions at m/z 299 (loss of CH₃ radical), m/z 284 (loss of CH₃ radical from m/z 299), m/z 282 (loss of CH₃OH from m/z 314), m/z 268 (loss of OCH₃ radical from m/z 299), m/z 151 (loss of C₈H₇N₂O₂ radical), m/z 150 (loss of C₈H₈N₂O₂) and m/z 120 (loss of CH₂O from m/z 150). The product ions at m/z 268, m/z 149, m/z 151, m/z 150 and m/z 120 are diagnostic ions for the proposed structure of OMP-4. (**Supplementary Scheme. Scheme.S5, Figure S2(a), Table. S3, see Supporting Information**) Based on these data OMP-4 was identified as 5-

1
2
3 methoxy-2-9(4-methoxy-3,5-dimethyl-2-methylenepyridin-2-yl)-methoxy)-1*H*-
4
5 benzo[*d*]imidazole.

6
7
8 **OMP-5 ([M+H]⁺, m/z 312.1337)**

9
10 The acidic and neutral hydrolytic degradation product OMP-5 at m/z 312 ([M+H]⁺) with an
11 elemental composition C₁₇H₁₈N₃O₅⁺ was eluted at 18.66 min. The LC-MS/MS spectrum of
12 [M+H]⁺ of OMP-5 showed high abundance product ions at m/z 269 (loss of CH₃ radical from
13 m/z 284), m/z 254 (loss of CH₃ radical from m/z 269) and low abundant product ions at m/z 297
14 (loss of CH₃ radical), m/z 296 (loss of CH₄), m/z 284 (loss of CO), m/z 280 (loss of CH₃OH),
15 m/z 268 (loss of CH₄ from m/z 284), m/z 252 (loss of CH₃OH from m/z 284), m/z 241 (loss of
16 CO from m/z 269), m/z 240 (loss of CO from m/z 268), m/z 226 (loss of CH₄ from m/z 241),
17 m/z 215 (loss of C₂H₂ from m/z 241), m/z 198 (loss of CO from m/z 226), m/z 147 (loss of
18 C₆H₇N from m/z 240) and m/z 136 (loss of C₇H₄N₂ from m/z 252). The product at m/z 147 is
19 diagnostic ion for the presence of 6-methoxy-1*H*-benzo[*d*]imidazole moiety and the product ion
20 at m/z 136, which authenticates presence of 4-methoxy-3,5-dimethylpyridine in OMP-5.
21 Formation of product ion at m/z 284 by the loss CO supports the proposed structure of OMP-5.
22
23 **(Supplementary Scheme.S6, Figure. S2(b), Table.S4, see Supporting Information)** Based on
24 all these data, the structure of OMP-5 was proposed as shown in **Scheme. 1**.

25
26
27
28 **OMP-6 ([M+H]⁺, m/z 332.1052)**

29
30 The base hydrolytic degradation product OMP-6 at m/z 332 ([M+H]⁺) with an elemental
31 composition C₁₆H₁₈N₃O₃S⁺ was detected at 11.50 min. The LC-MS/MS spectrum of [M+H]⁺ of
32 OMP-6 showed high abundant product ion at m/z 184 (loss of 5-methoxy-1*H*-
33 benzo[*d*]imidazole) and low abundance ions at m/z 314 (loss of H₂O), m/z 238 (loss of C₆H₆O),
34 m/z 197 (loss of C₈H₉NO), m/z 179 (loss of C₈H₁₁NO₂), m/z 166 (loss of H₂O from m/z 184),
35
36
37
38
39
40
41
42
43
44
45
46
47
48
49
50
51
52
53
54
55
56
57
58
59
60

m/z 154 (loss of C₈H₆N₂OS), m/z 149 (loss of C₈H₉NO₂S) and m/z 137 (loss of OH radical from m/z 154). Formation of product ion at m/z 314 clearly indicates presence of free -OH group in OMP-6. The product ions at m/z 184 and m/z 149 were supports the proposed structure of OMP-6. **(Supplementary Scheme.S7, Figure S2(c), Table.S5, see Supporting Information)** Based on these data, OMP-6 was identified as 2-((5-methoxy-1*H*-benzo[*d*]imidazol-2-ylsulfinyl)methyl)-3,5-dimethylpyridine-4-ol.

OMP-7 ([M+H]⁺, m/z 181.0404)

The degradation product OMP-7 at m/z 181 ([M+H]⁺) with an elemental composition C₂₂H₂₇FN₃O₆⁺ was detected at 13.05 min in base hydrolytic condition. The LC-MS/MS spectrum of [M+H]⁺ of OMP-7 showed high abundance product ions at m/z 166 (loss of CH₃ radical), m/z 138 (loss of CO from m/z 166) and low abundance product ions at m/z 165 (loss of CH₃OH), m/z 150 (loss of 'O' atom from m/z 166), m/z 149 (loss of 'S' atom), m/z 148 (loss of SH radical) and m/z 133 (loss of SH radical from m/z 166). The product ions at m/z 148 and m/z 149 are authenticate presence of free -SH group at imidazole carbon. Based on these data, OMP-7 was identified as 5-methoxy-1*H*-benzo[*d*]imidazole-2-thiol. **(Supplementary Scheme.S8,**

Figure S2(d), Table.S5, see Supporting Information)

OMP-8 ([M+H]⁺, m/z 316.1094)

The degradation product OMP-8 at m/z 316 ([M+H]⁺) with an elemental composition C₁₆H₁₈N₃O₂S⁺ detected at 14.07 min in base and neutral hydrolytic conditions. The decrease of 30 Da in molecular weight compared to [M+H]⁺ of the drug suggests that OMP-8 was formed by loss of 'CH₂O' molecule from the drug. The LC-MS/MS spectrum of [M+H]⁺ of OMP-8 showed high abundance product ion at m/z 168 (loss of 5-methoxy-1*H*-benzo[*d*]imidazole) and low abundance ions at m/z 301 (loss of CH₃ radical), m/z 284 (loss of OH radical from m/z 301) and m/z 149 (loss of C₈H₉NOS). The product ions at m/z 168 and m/z 149 are characteristic ion for

the proposed structure of OMP-8. The diagnostic product ion at m/z 149 authenticates presence of OCH_3 group on imidazole ring. (**Supplementary Scheme.S9, Figure S3(a), Table.S5, see Supporting Information**). Based on these data OMP-8 was identified as 5-methoxy-2-((3,5-dimethylpyridin-2-yl)methylsulfinyl)-5-methoxy-1*H*-benzo[*d*]imidazole.

OMP-9 ([M+H]⁺, m/z 180.1016)

The degradation product OMP-9 at m/z 180 ([M+H]⁺) with an elemental composition $\text{C}_{10}\text{H}_{14}\text{NO}_2^+$ was detected at 18.29 min in base hydrolysis conditions. The LC-MS/MS spectrum of [M+H]⁺ of OMP-9 showed highly abundance product ions at m/z 137 (loss of CH_3 radical from m/z 152) and low abundance product ions at m/z 164 (loss of CH_4), m/z 152 (loss of CO), m/z 150 (loss of CH_2O), m/z 136 (loss of CO from m/z 164) and m/z 108 (loss of CO from m/z 136). The significant product ions at m/z 152 and m/z 108 indicate presence of free carbonyl group at pyridine nitrogen. (**Supplementary Scheme.S10, Figure S3(b), Table.S6, see Supporting Information**) Based on these data OMP-9 was identified as 4-methoxy-3,5-dimethyl-2-methylene pyridine-1(2*H*)-carbaldehyde.

OMP-10 ([M+H]⁺, m/z 198.0576)

The degradation product OMP-10 at m/z 198([M+H]⁺) with an elemental composition $\text{C}_9\text{H}_{12}\text{NO}_2\text{S}^+$ was detected at 20.68 min in base hydrolytic condition. The ESI/MS/MS spectrum of [M+H]⁺ of OMP-10 showed intense product ions at m/z 180 (loss of H_2O) and low intense product ions at m/z 181 (loss of OH radical), m/z 166 (loss of CH_3 radical from m/z 181) and m/z 150 (loss of SO group). The product ions at m/z 181 and m/z 180 indicates presence of free $-\text{OH}$ group in OMP-10. The product ion at m/z 150 clearly indicates presence of free $-\text{S-OH}$ group in OMP-10. (**Supplementary Scheme.S11, Figure S3(c), Table.S6, see Supporting**

Information). Based on these data OMP-10 was identified as (z)-((4-methoxy-5-methyl-3-methylenepyridin-2(3*H*)-ylidene) methyl)sulfanol.

OMP-11 ([M+H]⁺, m/z 314.1138)

The neutral hydrolysis degradation product OMP-11 at m/z 314 ([M+H]⁺) with an elemental composition C₁₆H₁₆N₃O₄⁺ detected at 10.66 min. The LC-MS/MS spectrum of [M+H]⁺ of OMP-11 showed high abundance product ion at m/z 270 (loss of CO₂) and low abundance product ions at m/z 296 (loss of H₂O), m/z 268 (loss of CO from m/z 296), m/z 255 (loss of CH₃ radical from m/z 270), m/z 149 (loss of C₈H₇NO₃) and m/z 122 (loss of C₈H₆N₂O from m/z 268). Formation of diagnostic product ion at m/z 270 by the loss of CO₂ clearly indicates presence of –COOH group on OMP-11. The product ions at m/z 268, m/z 149 and m/z 122 supports the proposed structure of OMP-11. (**Supplementary Scheme.S12, Figure S3(d), Table.S7, see Supporting**

Information) Based on these data, OMP-11 was identified as 1-(6-methoxy-1*H*-benzo[*d*]imidazole-2-yl)-5-methyl-3-methylene-4-oxo-1,2,3,4-tetrahydropyridine-2-carboxylic.

OMP-12 ([M+H]⁺, m/z 284.1378)

The degradation product OMP-12 at m/z 284 ([M+H]⁺) with an elemental composition C₁₆H₁₈N₃O₂⁺ detected at 14.70 min in neutral hydrolytic degradation condition. The LC-MS/MS spectrum of [M+H]⁺ of OMP-12 showed high abundance product ions at m/z 269 (loss of CH₃ radical), m/z 254(loss of CH₃ radical from m/z 269) and low abundance product ion at m/z 268(loss of CH₄), m/z 147 (loss of C₈H₁₁NO), m/z 136 (loss of C₇H₄N₂O from m/z 268) and m/z 108 (loss of CO from m/z 136). The product ions at m/z 108, m/z 136 and m/z 147 clearly indicates ‘O’ forms bridge between 6-methoxy-1*H*-benzo[*d*]imidazole ring and 2,3,5-trimethylpyridine moiety in OMP-12. Formation of diagnostic product ion at m/z 147 authenticates presence of OCH₃ group on imidazole ring. (**Supplementary Scheme.S13, Figure**

S4(a), Table.S7, see Supporting Information) Based on these data, OMP-12 was identified as 2-((3,5-dimethylpyridin-2-yl)methoxy)-5-methoxy-1*H*-benzo[*d*]imidazole.

OMP-13 ([M+H]⁺, m/z 300.1341)

The neutral hydrolytic degradation product OMP-13 at m/z 300([M+H]⁺) with an elemental composition C₁₆H₁₈N₃O₃⁺ was detected at 23.17 min. The LC-MS/MS spectrum of [M+H]⁺ of OMP-13 showed high abundance product ion at m/z 270 (loss of CH₃ radical from m/z 285) and low abundance product ions at m/z 285 (loss of CH₃ radical), m/z 272 (loss of CO), m/z 257 (loss of CO from m/z 285), m/z 242 (loss of CH₃ from m/z 257), m/z 225 (loss of OH radical from m/z 242) and 173 (loss of C₄H₄ from m/z 225). The diagnostic product ion at m/z 173 indicates 'O' forms bridge between 6-methoxy-1*H*-benzo[*d*]imidazole ring and 2,3,5-trimethylpyridine-4-ol moiety in OMP-13. **(Supplementary Scheme.S14, Figure S4(b), Table.S8, see Supporting Information)** Based on these data, OMP-13 was identified as 2-((6-methoxy-1*H*-benzo[*d*]imidazol-2-yl)oxy)methyl)-3,5-dimethylpyridin-4-ol.

OMP-14 ([M+H]⁺, m/z 298.1174)

The degradation product OMP-14 at m/z 298 ([M+H]⁺) with an elemental composition C₁₆H₁₆N₃O₃⁺ detected at 23.97 min in neutral hydrolysis conditions. The LC-MS/MS spectrum of [M+H]⁺ of OMP-14 showed high abundance product ion at m/z 254 (loss of CO from m/z 282) and low abundance product ions at m/z 283 (loss of CH₃ radical), m/z 282 (loss of CH₄), m/z 270 (loss of CO), m/z 240 (loss of CH₃ radical from m/z 255), m/z 224 (loss of 'O' from m/z 240) and m/z 173 (loss of C₄H₃ radical from m/z 224). The product ions at m/z 270 indicates presence of carbonyl moiety in OMP-14 and the product ion at m/z 173 is diagnostic ion for the proposed structure of OMP-14. **(Supplementary Scheme.S15, Figure S4(c), Table.S8, see**

Supporting Information) Based on these data OMP-14 was identified as 2-((6-methoxy-1*H*-benzo[*d*]imidazole-2-yl)oxy)methyl)-5-methyl-3-methylenepyridin-4(3*H*)-one.

OMP-15 ([M+H]⁺, m/z 362.1152)

The oxidative degradation product OMP-15 at m/z 362 ([M+H]⁺) with an elemental composition C₁₇H₂₀N₃O₄S⁺ detected at 20.02 min. The increase of 16 Da in molecular weight compared to the [M+H]⁺ of the drug suggests that OMP-15 was oxidative degradation product. The LC-MS/MS spectrum of [M+H]⁺ of OMP-15 at m/z 362 showed high abundance product ion at m/z 150 (loss of 'O' from m/z 166) and low abundant product ions at m/z 298 (loss of SO₂), m/z 283 (loss of CH₃ radical from m/z 298), m/z 268 (loss of CH₂O from m/z 298), m/z 268 (loss of CH₃ radical from m/z 283), m/z 266 (loss of OH radical from m/z 283), m/z 240 (loss of CO from m/z 268), m/z 214 (loss of C₈H₈N₂O), m/z 195 (loss of C₉H₁₃NO₂), m/z 179 (loss of 'O' from m/z 195) and m/z 168 (loss of C₈H₆N₂O₂S). The product ions at m/z 214, m/z 195 and m/z 168 clearly indicates oxidation takes place at sulfoxide of the drug. (**Supplementary Scheme.S16, Figure S4(d), Table.S9, see Supporting Information**) Based on these data OMP-15 was identified as 5-methoxy-2-((4-methoxy-3,5-dimethylpyridin-2-yl) methylsulfonyl)-1*H*-benzo[*d*]imidazole..

OMP-16 ([M+H]⁺, m/z 378.1102)

The oxidative degradation product OMP-16 at m/z 362 ([M+H]⁺) with an elemental composition C₁₇H₂₀N₃O₄S⁺ detected at 15.14 min. The increase of 32 Da in molecular weight compared to the [M+H]⁺ of the drug suggests that OMP-16 was di oxidative degradation product. The LC-MS/MS spectrum of [M+H]⁺ of OMP-16 showed high abundance product ion at m/z 150 (loss of 'O' from m/z 166) and low abundance product ions at m/z 314 (loss of SO₂), m/z 299 (loss of CH₃ radical from m/z 314), m/z 211 (loss of C₉H₁₃NO₂), m/z 183 (loss of C₁₀H₁₄NO₃) and m/z 168 (loss of C₈H₆N₂O₃S). The product ions at m/z 314, m/z 211 and m/z 168 support the

1
2
3 proposed structure of OMP-16. (**Supplementary Scheme.S17, Figure S4(e), Table.S9, see**
4 **Supporting Information**). All these data are consistent with the structure, 4-methoxy-2-((5-
5 methoxy-1*H*-benzo[*d*]imidazole-2-ylsulfonyl)methyl-3,5-dimethylpyridine 1-oxide which has
6 been proposed for OMP-16.
7
8
9
10

11 **5. Mechanistic pathway for the formation of degradation products**

12 **5.1 Hydrolytic degradation condition**

13
14
15
16
17 1. The degradation product OMP-1, formed by loss of 'O' from the drug under acidic conditions
18 may involve a radical cation mechanism [35] . Formation of OMP-2 and OMP-3 can be
19 explained by abstraction of an acidic proton by 'N' of the imidazole ring followed nucleophilic
20 attack of pyridine leading to cleavage of C-S bond to form an intermediate with free S-OH
21 group. The consecutive losses of 'SO' and H₂O molecules can lead to the formation of OMP-1
22 and OMP-3, respectively. Formation of OMP-4 can be explained by sulfoxide oxygen forms
23 new O-C bond with the imidazole carbon followed by the loss of 'S' leads to form OMP-4. The
24 degradation product OMP-4 further abstracts acidic proton followed by participation of
25 rearrangement leads to form OMP-5. (**Supplementary Scheme. S18, see Supporting**
26 **Information**)
27
28

29
30
31
32
33 2. In the case of base hydrolysis the base OH⁻ ion abstracts the proton from the OMP followed
34 by hydrolysis leads to form OMP-6, OMP-7 and OMP-8. Formation of OMP-9 can be explained
35 by OH⁻ ion abstracts the proton followed by nucleophilic attack of pyridine aleading to cleavage
36 of C-S bond. After which may undergo hydrolysis leads to form OMP-9 and OMP-10.
37
38 (**Supplementary Scheme. S18, see Supporting Information**)
39

40
41
42
43
44 3. Loss of 'S' atom from the OMP followed by loss of CH₂O and CH₄ molecules leads to form
45 OMP-12 and OMP-14 in neutral hydrolytic reaction. The degradation product OMP-14, which
46 may participates in neutral hydrolysis reaction leads to form OMP-11. The degradation product
47
48
49
50
51
52
53
54
55
56
57
58
59
60

OMP-8 was formed by loss of CH₂O molecule and formation of OMP-13 was explained by loss of 'O' atom followed by loss of CH₂O leads to form OMP-13. (**Supplementary Scheme. S19, see Supporting Information**).

5.2. Oxidative degradation condition

Formation of oxidative degradation product **OMP-15** can be explained by nucleophilic attack of peroxide on sulfoxide of the drug of the drug followed by loss of H₂O molecule leads to form **OMP-15**. This degradation product OMP-15 further oxidised by H₂O₂ leads to form **OMP-16** (**Supplementary Scheme. S19, see Supporting Information**).

6. Synthesis and NMR studies of oxidative degradation products

6.1. Procedure for synthesis of OMP-15 and OMP-16

For the synthesis of OMP-15 and OMP-16, 1 mmol and 2 mmol *m*-CPBA (172mg, 344mg) respectively was added separately to each of the two solutions of OMP (346 mg, 1 mmol) in 3ml of DCM. Mixture of the reaction was stirred for overnight at room temperature. After the completion of the reaction, the sample mixture was quenched with NaHCO₃ followed by extraction with ethyl acetate (15 ml) and separated organic layer to be collected. The collected sample was dried over on anhydrous magnesium sulfate and concentrated under vacuum to get dry product. The sample residue was purified with silica gel column chromatography (DCM–MeOH, 9.5:0.5 %) to afford pure products OMP-15 and OMP-16 as solid. Then the pure solid compounds were subjected to 1D and 2D NMR experiment studies. Based on the NMR experiments, structures of OMP-15 and OMP-16 were confirmed (**Supplementary Figure S5-S13, see Supporting Information**). (**Scheme 1**).

6.2. Structural elucidation of OMP-15 and OMP-16 by NMR experiments

¹H NMR (1D and 2D) experiments, were performed on a 400 MHz (Avance 400 MHz, Bruker)

spectrometer using CD₃OD as a solvent. Chemical shift values were reported on delta scale in ppm using solvent residual signal as internal standard.

Structures were fully characterized based on extensive analysis of 1D and 2D NMR experiments including 2-D Double Quantum Filtered Correlation Spectroscopy (DQF-COSY), Nuclear Overhauser Effect Spectroscopy (NOESY), Heteronuclear-Single Quantum correlation (HSQC) and Heteronuclear-multiple Quantum correlation (HMBC) experiments. Molecular formula of protonated OMP-15 was deduced as C₁₇H₁₉N₃O₄S by HRMS .

The distinctive singlet at 7.98 ppm in OMP-15 due to H13 was used to initiate the assignments with the help of DQF-COSY and NOESY experiments. The chemical shift at δ 2.20 ppm was assigned to 14-CH₃ with the help of strong nOe correlation, H13/14-CH₃ (δ 2.20 ppm). The remaining methyl, 16-CH₃ and 15-OCH₃ appeared at δ 2.19 and δ 3.69 ppm. In addition the nOe correlations, 14-CH₃/15-OCH₃ and 15-OCH₃/16-CH₃ provide further affirmation. It was easy to distinguish H1 and H6 protons observed as double doublet at δ 7.01 and doublet δ 7.55 ppm, respectively. The close proximity of H1/2-OCH₃, supporting to fixed as 2-OCH₃ at δ 3.84 ppm. The HRMS and the NMR spectroscopic data adequately support the proposed structure of OMP-15. (Figure.3)

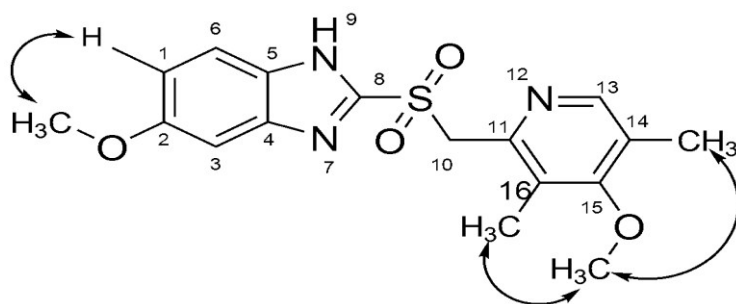


Figure.3: The structure of OMP-15 along with the characteristic NOE correlations represented as double headed arrows.

The molecular formula of OMP-16 (m/z 378 $[M+H]^+$) was deduced as $C_{17}H_{19}N_3O_5S$ by HRMS. Its NMR data were similar to those of OMP-15, indicating the presence of an identical moiety. The chemical shifts (**Supplementary Table S10, see Supporting Information**) of protons varying due to the presence of additional oxygen atom and the HRMS and NMR spectroscopic data adequately supports the proposed structure of OMP-16 as shown in the Figure.4. (**Supplementary Table S11, see Supporting Information**)

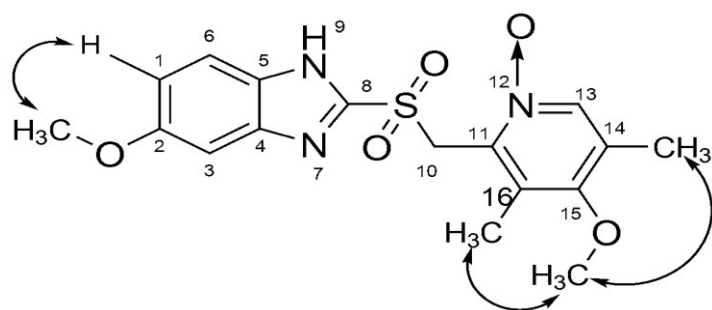


Figure.4: The structure of OMP-16 along with the characteristic NOE correlations represented as double headed arrows.

7. MTT ASSAY

All the test compounds were treated to two different normal cells. The standard OMP was found to be more toxic compared to OMP-15 and OMP-16. In standard OMP, where, 50% inhibition of cells were noticed at 32.85 μg and 28.21 μg in HEK-29 and NIH3T3 cell lines. In case of OMP-15, it was found to be at 62.70 μg and 56.40 μg and for OMP-16 at 57.05 μg and 63.76 μg in HEK-29 and NIH3T3 cell lines. However, when compared to the standard OMP, both OMP-15 and OMP-16 were found to have relatively lesser toxic effects towards normal cells.

(**Supplementary Table S12, see Supporting Information**)

8. *In silico* toxicity studies

The potential toxicity of OMP and its degradation products were assessed by ProTox-II [36]. It predicts toxicity of chemicals into different levels such as oral toxicity, organ toxicity (hepatotoxicity), toxicological endpoints (such as mutagenicity, carcinotoxicity, cytotoxicity and immunotoxicity), toxicological pathways and toxicity targets.

The predicted toxicity of the molecule having data point with a confidence below 70% are omitted whereas active predicted target with the input molecule are shown in bold predicted tag. The toxicity results of input molecule of OMP and its degradation products are shown in the **Table.2((A),(B),(C))**. Organ toxicity, hepato toxicity, of OMP-7 is predicted with confidence score 0.74 and the toxicological endpoint, carcinogenicity, of OMP and OMP-8 are predicted with confidence score 0.81 and 0.79. The degradation products OMP-2, OMP-3, OMP-9, OMP-11, OMP-14 and OMP-16 have adverse effects on the immune system are predicted with confidence score 0.99, 0.97, 0.86, 0.94, 0.98 and 0.92. Tox21 Nuclear receptor signaling pathways, aryl hydro carbon receptor(AhR), of OMP, OMP-1, OMP-6, OMP-7, OMP-8, OMP-13 and OMP-15 are predicted with confidence score 1, 0.74, 0.83, 0.74, 0.98, 0.73 and 0.85. Additionally, two different targets, Prostaglandin G/H Synthase 1 and Amine Oxidase A are predicted as toxicity targets for OMP, OMP-1, OMP-6, OMP-8, OMP-13, OMP-15 and OMP-16, DP-3, DP-4 and DP-6 with probable binding. ProTox-II provides insight that there is a feasibility that OMP degradation products can be active for multiple toxicity endpoint and thereby resulting in severe toxic effects.

Table 2(A): Toxicity prediction of OMP and its degradation products

Classification	Target	OMP and its degradation products					
		OMP	OMP-1	OMP-2	OMP-3	OMP-4	OMP-5
Toxicity Class		4	5	4	2	4	4
Predicted LD50	Oral toxicity	1400mg/kg	5000mg/kg	330mg/kg	33mg/kg	1250mg/kg	840mg/kg
Organ toxicity	Hepatotoxicity	Inactive	Inactive	Inactive	Inactive	Inactive	Inactive
Toxicity end points	Carcinogenicity	Active^{1a}	Inactive	Inactive	Inactive	Inactive	Inactive
Toxicity end points	Immunotoxicity	Inactive	Inactive	Active³	Active⁴	Inactive	Inactive
Toxicity end points	Mutagenicity	Inactive	Inactive	Inactive	Inactive	Inactive	Inactive
Toxicity end points	Cytotoxicity	Inactive	Inactive	Inactive	Inactive	Inactive	Inactive
Tox21-Nuclear receptor signaling pathways	Aryl hydrocarbon Receptor (AhR)	Active^{1b}	Active²	Inactive	Inactive	Inactive	Inactive
Tox21-Nuclear receptor signaling pathways	Androgen Receptor (AR)	Inactive	Inactive	Inactive	Inactive	Inactive	Inactive
Tox21-Nuclear receptor signaling pathways	Androgen Receptor Ligand Binding Domain (AR-LBD)	Inactive	Inactive	Inactive	Inactive	Inactive	Inactive
Tox21-Nuclear receptor signaling pathways	Aromatase	Inactive	Inactive	Inactive	Inactive	Inactive	Inactive
Tox21-Nuclear receptor signaling pathways	Estrogen Receptor Alpha (ER)	Inactive	Inactive	Inactive	Inactive	Inactive	Inactive
Tox21-Nuclear receptor signaling pathways	Estrogen Receptor Ligand Binding Domain (ER-LBD)	Inactive	Inactive	Inactive	Inactive	Inactive	Inactive
Tox21-Nuclear receptor signaling pathways	Peroxisome Proliferator Activated Receptor Gamma (PPAR-Gamma)	Inactive	Inactive	Inactive	Inactive	Inactive	Inactive
Tox21-Stress response pathways	Nuclear factor (erythroid-derived 2)-like 2/antioxidant responsive element (nrf2/ARE)	Inactive	Inactive	Inactive	Inactive	Inactive	Inactive
Tox21-Stress response pathways	Heat shock factor response element (HSE)	Inactive	Inactive	Inactive	Inactive	Inactive	Inactive
Tox21-Stress response pathways	Mitochondrial Membrane	Inactive	Inactive	Inactive	Inactive	Inactive	Inactive

		Potential (MMP)					
Tox21-Stress response pathways	Phosphoprotein (Tumor Suppressor) p53	Inactive	Inactive	Inactive	Inactive	Inactive	Inactive
Tox21-Stress response pathways	ATPase family AAA domain-containing protein 5 (ATAD5)	Inactive	Inactive	Inactive	Inactive	Inactive	Inactive
Toxicity Target		AOFA	AOFA	No binding	No binding	No binding	No binding
		PGH1	PGH1				

Table 2(B): Toxicity prediction of OMP and its degradation products

Classification	Target	OMP and its degradation products					
		OMP-6	OMP-7	OMP-8	OMP-9	OMP-10	OMP-11
Toxicity Class		4	4	5	4	4	5
Predicted LD50	Oral toxicity	1400mg/kg	500mg/kg	5000mg/kg	1000mg/kg	1000mg/kg	3200mg/kg
Organ toxicity	Hepatotoxicity	Inactive	Active ^{6a}	Inactive	Inactive	Inactive	Inactive
Toxicity end points	Carcinogenicity	Inactive	Inactive	Active ^{7a}	Inactive	Inactive	Inactive
Toxicity end points	Immunotoxicity	Inactive	Inactive	Inactive	Active ⁸	Inactive	Active ⁹
Toxicity end points	Mutagenicity	Inactive	Inactive	Inactive	Inactive	Inactive	Inactive
Toxicity end points	Cytotoxicity	Inactive	Inactive	Inactive	Inactive	Inactive	Inactive
Tox21-Nuclear receptor signaling pathways	Aryl hydrocarbon Receptor (AhR)	Active ⁵	Active ^{6b}	Active ^{7b}	Inactive	Inactive	Inactive
Tox21-Nuclear receptor signaling pathways	Androgen Receptor (AR)	Inactive	Inactive	Inactive	Inactive	Inactive	Inactive
Tox21-Nuclear receptor signaling pathways	Androgen Receptor Ligand Binding Domain (AR-LBD)	Inactive	Inactive	Inactive	Inactive	Inactive	Inactive
Tox21-Nuclear receptor signaling pathways	Aromatase	Inactive	Inactive	Inactive	Inactive	Inactive	Inactive
Tox21-Nuclear receptor signaling pathways	Estrogen Receptor Alpha (ER)	Inactive	Inactive	Inactive	Inactive	Inactive	Inactive

Tox21-Nuclear receptor signaling pathways	Estrogen Receptor Ligand Binding Domain (ER-LBD)	Inactive	Inactive	Inactive	Inactive	Inactive	Inactive
Tox21-Nuclear receptor signaling pathways	Peroxisome Proliferator Activated Receptor Gamma (PPAR-Gamma)	Inactive	Inactive	Inactive	Inactive	Inactive	Inactive
Tox21-Stress response pathways	Nuclear factor (erythroid-derived 2)-like 2/antioxidant responsive element (nrf2/ARE)	Inactive	Inactive	Inactive	Inactive	Inactive	Inactive
Tox21-Stress response pathways	Heat shock factor response element (HSE)	Inactive	Inactive	Inactive	Inactive	Inactive	Inactive
Tox21-Stress response pathways	Mitochondrial Membrane Potential (MMP)	Inactive	Inactive	Inactive	Inactive	Inactive	Inactive
Tox21-Stress response pathways	Phosphoprotein (Tumor Suppressor) p53	Inactive	Inactive	Inactive	Inactive	Inactive	Inactive
Tox21-Stress response pathways	ATPase family AAA domain-containing protein 5 (ATAD5)	Inactive	Inactive	Inactive	Inactive	Inactive	Inactive
Toxicity Target		AOFA PGH1	No binding	AOFA PGH1	No binding	No binding	No binding

Table 2(C): Toxicity prediction of OMP and its degradation products

Classification	Target	OMP and its degradation products				
		OMP-12	OMP-13	OMP-14	OMP-15	OMP-16
Toxicity Class		4	5	4	4	4
Predicted LD50	Oral toxicity	500mg/kg	5000mg/kg	780mg/kg	1400mg/kg	1400mg/kg
Organ toxicity	Hepatotoxicity	Inactive	Inactive	Inactive	Inactive	Inactive
Toxicity end points	Carcinogenicity	Inactive	Inactive	Inactive	Inactive	Inactive
Toxicity end points	Immunotoxicity	Inactive	Inactive	Active¹¹	Inactive	Active¹³
Toxicity end points	Mutagenicity	Inactive	Inactive	Inactive	Inactive	Inactive
Toxicity end points	Cytotoxicity	Inactive	Inactive	Inactive	Inactive	Inactive
Tox21-Nuclear receptor signaling	Aryl hydrocarbon Receptor (AhR)	Inactive	Active¹⁰	Inactive	Active¹²	Inactive

pathways						
Tox21-Nuclear receptor signaling pathways	Androgen Receptor (AR)	Inactive	Inactive	Inactive	Inactive	Inactive
Tox21-Nuclear receptor signaling pathways	Androgen Receptor Ligand Binding Domain (AR-LBD)	Inactive	Inactive	Inactive	Inactive	Inactive
Tox21-Nuclear receptor signaling pathways	Aromatase	Inactive	Inactive	Inactive	Inactive	Inactive
Tox21-Nuclear receptor signaling pathways	Estrogen Receptor Alpha (ER)	Inactive	Inactive	Inactive	Inactive	Inactive
Tox21-Nuclear receptor signaling pathways	Estrogen Receptor Ligand Binding Domain (ER-LBD)	Inactive	Inactive	Inactive	Inactive	Inactive
Tox21-Nuclear receptor signaling pathways	Peroxisome Proliferator Activated Receptor Gamma (PPAR-Gamma)	Inactive	Inactive	Inactive	Inactive	Inactive
Tox21-Stress response pathways	Nuclear factor (erythroid-derived 2)-like 2/antioxidant responsive element (nrf2/ARE)	Inactive	Inactive	Inactive	Inactive	Inactive
Tox21-Stress response pathways	Heat shock factor response element (HSE)	Inactive	Inactive	Inactive	Inactive	Inactive
Tox21-Stress response pathways	Mitochondrial Membrane Potential (MMP)	Inactive	Inactive	Inactive	Inactive	Inactive
Tox21-Stress response pathways	Phosphoprotein (Tumor Suppressor) p53	Inactive	Inactive	Inactive	Inactive	Inactive
Tox21-Stress response pathways	ATPase family AAA domain-containing protein 5 (ATAD5)	Inactive	Inactive	Inactive	Inactive	Inactive
Toxicity Target		No binding	AOFA	No binding	AOFA	AOFA
			PGH1		PGH1	PGH1

Confidence Score: $1^a=0.81, 1^b=0.74, 3=0.99, 4=0.97, 5=0.83, 6^a=0.71, 6^b=0.74, 7^a=0.79, 7^b=0.98, 8=0.86$ and $9=0.94, 10=0.73, 11=0.98, 12=0.85, 13=0.92$

9. Conclusion

Forced degradation studies of OMP, carried out as per ICH guide lines, gave rise to a total of 16 degradation products which were characterized by LC-MS/MS in combination with accurate mass measurements. The oxidative degradation products OMP-15 and OMP-16 were synthesized and confirmed by 1D and 2D NMR experiments. Further the cytotoxic effects of degradation products were tested on normal human cells such as HEK 293 and NIH3T3 by MTT assay. From the results of cytotoxicity, both OMP-15 and OMP-16 were found to have relatively lesser toxic effects towards normal cells compared to OMP. Further, *in silico* toxicity of OMP and its degradation products were assessed by ProTox-II prediction tool. OMP and OMP-8 are predicted for carcinogenicity, OMP-7 for hepato toxicity and OMP-2, OMP-3, OMP-9, OMP-11, OMP-14 and OMP-16 for immune system with high confidence score. The drug, OMP-1, OMP-6, OMP-7, OMP-8, OMP-13 and OMP-15 are predicted to possess aryl hydro carbon receptor (AhR) with high probability score. Additionally, two different targets, Amine Oxidase A and Prostaglandin G/H Synthase 1 are predicted as toxicity targets for OMP, OMP-1, OMP-6, OMP-8, OMP-13, OMP-15 and OMP-16, DP-3, DP-4 and DP-6 with probable binding.

Acknowledgement

The authors thank Dr S Chandrasekhar, Director, IICT, Hyderabad for facilities and their cooperation. R Srinivas thanks CSIR emeritus project , ES1617Y5030 for partial financial support. G.S is thankful to CSIR, New Delhi, for awarding Junior Research Fellowship. R.M.B and S. U are thankful to CSIR, New Delhi, for awarding Senior Research Fellowship and Junior Research Fellowship, respectively.

Appendix A. Supplementary data

Supplementary data related to this article can be found at additional document

References

- [1] ICH guidelines, Q1A (R2): Stability Testing of New Drug Substances and Products (revision2), International Conference on Harmonization.
- [2] S. Singh, T. Handa, M. Narayanam, A. Sahu, M. Junwal, R. P. Shah. *J. Pharm. Biomed. Anal.* 2012, **69**, 148.
- [3] Chen G, Pramanik BN, Liu YH, Mirza UA. *J Mass Spectrum*, 2007, 42, 279-287.
- [4] B. Raju, M. Ramesh, R. Srinivas, S. S. Raju, Y. Venkateswarlu. *J. Pharm. Biomed. Anal.* 2011, **56**, 560.
- [5] R. M. Borkar, B. Raju, P. S. Devrukhakar, N. Tondepu, A. B. N. Rao, R. Srinivas. *RCM*, 2013, **27**, 369.
- [6] Prinesh N. Patel, Roshan M. Borkar, Pradipbhai D. Kalariya, Rahul P. Gangwal, c Abhay T. Sangamwar, Gananadhamu Samanthulaa and Srinivas Ragampeta. *J Mass Spectrum*, 2015, **50**(2), 344-53.
- [7] Deepak Namdev, Roshan M. Borkar, B. Raju, Pradipbhai D. Kalariya, Vinodkumar T. Rahangdale, S. Gananadhamu, R. Srinivas. *JPBA*, 2014, **88**, 245-255.
- [8] R. M. Borkar, B. Raju, R. Srinivas, S. K. Shetty. *Biomed. Chromatogr.* 2012, 26, 720.
- [9] Alsante KM, Baertschi SW. *Pharm Tech*, 2003, 60-72.
- [10] L.K. Zang, B.N. Pramanik. *J. Mass Spectrum*, 2010, **45**, 146.
- [11] ICH. Impurities in New Drug Products Q3B (R2). International Conference on Harmonisation, IFPMA: Geneva (Switzerland), 2006.
- [12] ICH. Impurities in New Drug Substances Q3A (R2). International Conference on Harmonisation. IFPMA: Geneva (Switzerland), 2006.

- 1
2
3 [13] Betto, L. Turchetto, L. Longinotti. *Annali Dell'Istituto Superiore di Sanità*, 1989, **25**, 315.
4
5
6
7 [14] N. Entwistle, P. Owen, D. Patterson, L. Jones, J. Smith. *J Forensic Sci Soc*, 1986, **26**, 45.
8
9
10 [15] L. Müller, R. J. Mauthe, C. M. Riley, M. M. Andino, D. D. Antonis, C. Beels, J. De
11 George, A. G. M. D. Knaep, D. Ellison, J. A. Fagerland, R. Frank, B. Fritschel, S.
12 Galloway, E. Harpur, C. D. N. Humfrey, A. S. Jacks, N. Jagota, J. Mackinnon, G.
13 Mohan, D. K. Ness, M. R. O'Donovan, M. D. Smith, G. Vudathala and L. Yotti, *Regul.*
14 *Toxicol. Pharmacol*, 2006, **44**, 198–211.
15
16 [16] G. Shankar, R. M. Borkar, U. Suresh, L. Guntuku, V. G. M. Naidu, N. Nageshc and R.
17 Srinivas. *J Mass Spectrum*, 2017, **52**, 459–471.
18
19 [17] Suresh Udutha, G Shankar, Roshan M Borkar, K Kumar GSrinivasulu, Lalitha Guntuku,
20 VGM Naidu, R Srinivas, *J Mass Spectrum*, 2018, **53**(10), 963-975.
21
22 [18] MM Bhandi, R.M Borkar, G Shankar, S Raut, N Nagesh, R Srinivas. *RSC Advances*,
23 2015, **6** (13), 10719-10735.
24
25 [19] Kennedy T, Jones R, *Aliment Pharmacol Ther*. 2000, **14**, 1589-1594.
26
27 [20] Locke GR 3rd, Talley NJ, Fett SL, Zinsmeister AR, Melton LJ 3rd. *Gastroenterology*,
28 1997, **112**, 1448-1456.
29
30 [21] Spechler SJ, *Epidemiology, Digestion*, 1992, **51**, 24-29.
31
32 [22] Orlando RC, *Am J Gastroenterol*, 1997, **92** , 3S-5S, discussion 5S-7S.
33
34 [23] A. Soni, R. E. Sampliner and A, Sonnenberg. *Am J Gastroenterol*, 2000, **95**(8), 1881–
35 1887.
36
37 [24] J. J. Caro, M. Salas, and A. Ward, *Clin Ther*, 2001, **23**(7), 998–1017.
38
39 [25] Howdern C.W, *Clin. Pharmacokinet*, 1990, **20**, 39-49.
40
41
42
43
44
45
46
47
48
49
50
51
52
53
54
55
56
57
58
59
60

- 1
2
3 [26] Sachs G, Shin JM, Howden CW. *Aliment Pharmacol Ther*, 2006, **23**, Suppl 2:2-8.
4
5 [27] E. C. Klinkenberg-Knol, F. Nelis, J. Dent et al, *Gastroenterology*, 2000, **118**(4), 661–
6
7 669.
8
9 [28] Raja Kumar Seshadri, Thummala Veera Raghavaraju and Ivon Elisha Chakravarthy. *Sci*
10
11 *Pharm*, 2013, **81**(2), 437–458.
12
13 [29] Castro D., Moreno M. A., Torrado S. and Lastres J. L, *JPBA*, 1999, **2** (21), 291-298.
14
15 [30] Mathew M., Gupta V., Baily R. E. *Ind. Pharm*, 1995, **21**, 965-971.
16
17 [31] Ahmad, L.; Iqbal, Z.; Nazir, S.; Shah, Y.; Khan, A.; Khan, M. I.; Nasir, F.; Khan, J.
18
19 *Liquid Chromatogr. Rel. Technol*, 2011, **34** (15), 1488–1501.
20
21 [32] Kanazawa, H.; Okada, A.; Matsushima, Y.; Yokota, H.; Okubo, S.; Mashige, F.;
22
23 Nakahara, K, *J. Chromatogr. A*. 2002, **949** (1), 1–9.
24
25 [33] Wang, J.; Wang, Y.; Fawcett, J. P.; Wang, Y.; Gu, J. *JBPA*, 2005, **39**(3), 631–635.
26
27 [34] Bollu VS, Nethi SK, Dasari RK, Rao SS, Misra S, Patra CR. *Nanotoxicology*,
28
29 2016, **10**(4), 413-25.
30
31 [35] B.Satyanarayana, P. Vasudev. *Am J Analyt Chem*, 2015, **6**, 145.
32
33
34
35
36
37
38
39 [36] Banerjee P, Eckert AO, Schrey AK, Preissner R. *ProTox-II*, *Nucleic Acids Res*, 2018.
40
41
42
43
44
45
46
47
48
49
50
51
52
53
54
55
56
57
58
59
60